Supplemental Section

B. R. Tuttle et al., Journal of Physics and Chemistry of Solids 208, 113190 (Supp. Mat.) (2026)

Table S0: Convergence Test Results calculated using a 1x2x1 supercell: Column 1 includes the planewave cutoff (E_c), column 2 is the bulk total energy (E_{bulk}^{tot}), column 3 is the total relaxed energy of an iodine vacancy (E_{Vac}^{tot}), column 4 is the energy difference $\Delta E = E_{Vac} - E_{tot}^{bulk}$, column 5 is the band gap E_{gap} for the bulk crystal. As illustrated, while the total energies do not converge until $E_c = 380\ eV$, the physical properties of interest ΔE and E_{gap} are well converged for $E_c = 220\ eV$.

1	2	3	4	5
$E_c\ (eV)$	$E_{bulk}^{tot}\ (eV)$	$E_{Vac}^{tot}\ (eV)$	$\Delta E\ (eV)$	$E_{gap}\ (eV)$
140	−253.72	−251.09	+2.63	1.83
220	−253.06	−250.45	+2.61	1.81
300	−253.01	−250.40	+2.61	1.81
380	−252.98	−250.37	+2.61	1.81
460	−252.98	−250.37	+2.61	1.81

Figure S0. Supercell Structure: Ball and stick representation of the 2x3x1 supercell of $Rb_3Sb_2I_9$ in the (a) plane of (a, c) and (b) in the plane of (a, b) and (c) in the (b, c) plane. Large pink balls are rubidium atoms, the small gold balls are antimony, and the small purple balls are iodine.

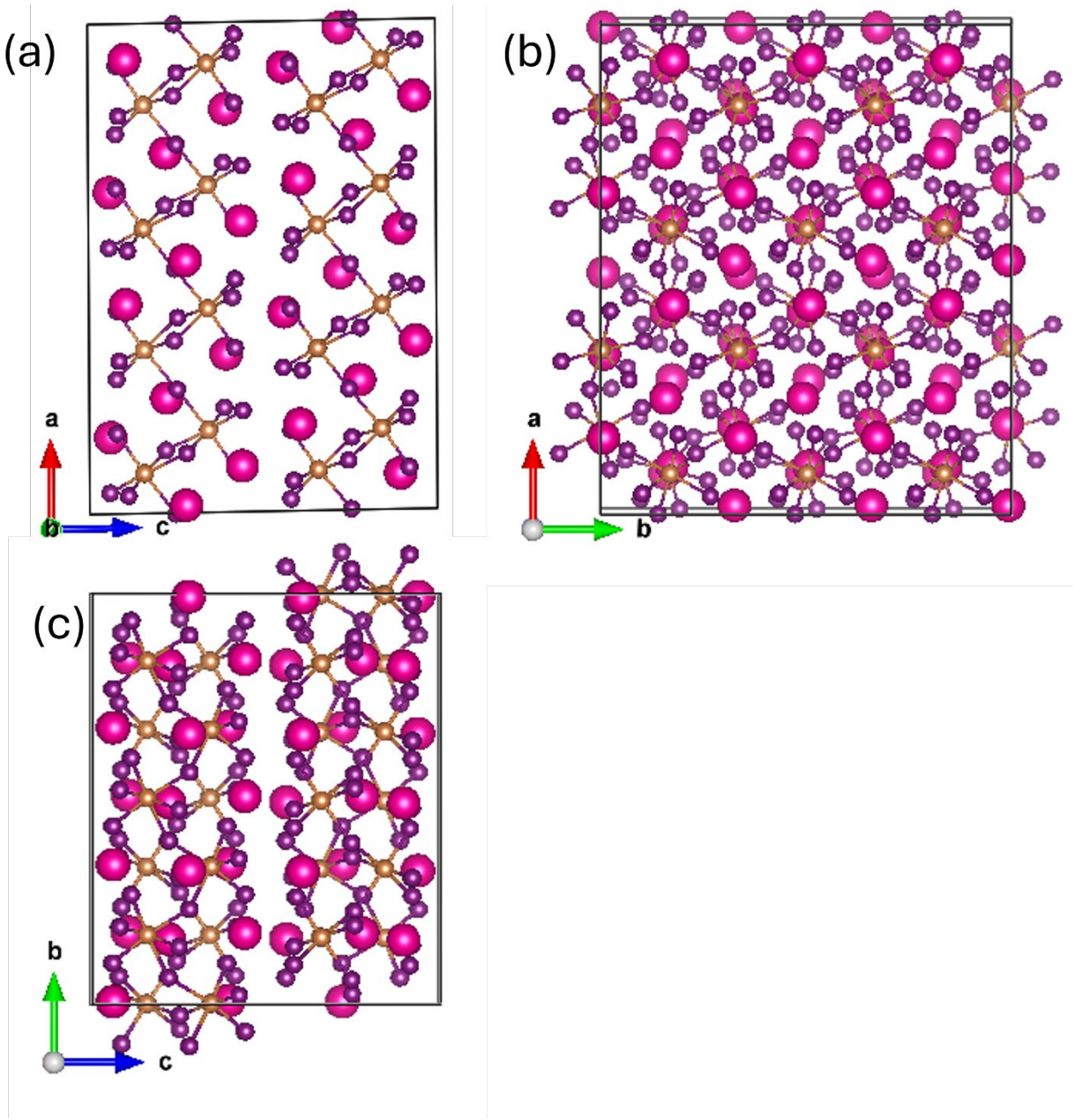
(a)
a
b
c
(b)
a
b
(c)
b
c

S1. convergence, uncertainties

a. Periodic Cell Approximation

Using finite supercells leads to some uncertainty in the formation energies reported below. Using finite supercells leads to a defect interacting with its periodic image which is ~ 20 Å away. In experiments, the defects are dilute with more than 100 Å between them. For our supercell calculations, periodic interactions affect the atomic relaxations and the electronic properties. To estimate the size of finite cell effects on formation energies, we can compare 1x2x1 supercell with 2x3x1 supercell formation energy (E_{form}) results, which can be extracted from Figures 7 and 8(a). In Table S1, we explicitly report E_{form} for the case where the Fermi energy is at the valence band maximum and the formation energy is low (< 2 eV). The average absolute difference between the formation energies (ΔE_{form}) is 0.038 eV indicating that the 2x3x1 results are numerically converged with respect to cell size to less than 0.04 eV.

Table S1: The defect symbol, charge state (Q), the formation energies (E_{form}) and the energy difference (ΔE_{form}) are reported for 5 types of defects.

Defect	Q	E_f (eV) 1x2x1	E_f (eV) 2x3x1	ΔE_{form} (eV)
Va_{I1}	0	1.18	1.20	+0.02
Va_{I1}	−1	2.78	2.82	+0.04
Va_{I1}	+1	−0.14	−0.13	+0.01
Va_{I2}	0	1.69	1.63	−0.06
Va_{I2}	+1	0.04	0.03	−0.01
Va_{Rb}	0	1.28	1.23	−0.06
Va_{Rb}	−1	1.61	1.53	−0.08
Va_{Rb}	+1	1.11	1.07	−0.04
Rb_{i1}	0	1.57	1.62	+0.05
Rb_{i1}	+1	−0.26	−0.23	+0.03
Rb_{i1}	+2	−0.32	−0.33	−0.01
Rb_{i2}	0	1.63	1.60	−0.03
Rb_{i2}	+1	−0.26	−0.28	−0.02
Rb_{i2}	+2	−0.30	−0.39	−0.09

As mentioned in the introduction, methods have been employed to extract the dilute limit for the periodic correction of charged defects. One uncertainty in this process can be found from the potential alignment term (ΔV). As shown from the green dots in Figure S1, the ΔV term is calculated by subtracting the actual variation of the electrostatic potential to that of a model charge as calculated at each atom in the supercell. Below, we show a plot for 2x3x1 supercell result for a rubidium vacancy in the $q = 2$ state. The value of ΔV is found by averaging the values for the last 30 % of data points where there is convergence. The standard deviation from the average gives an estimate of one contribution to the uncertainty in the formation energy results. A numerical uncertainty can be calculated by the average of $|q\Delta V_{st,dev}|$ over all charged defects which is 0.052 eV. The calculation

of E_{lum}^{th} and E_{PICT}^{th} involves only $q = \pm 1$ for iodine vacancies; averaging $|q\Delta V_{st,dev}|$ over defects in these charge states gives 0.021 eV. We find that using a 1x2x1 supercell results standard deviations $2-3$ times as large.

Figure S1: The atom localized electrostatic potential is plotted versus distance for the rubidium vacancy. See text above for more details.

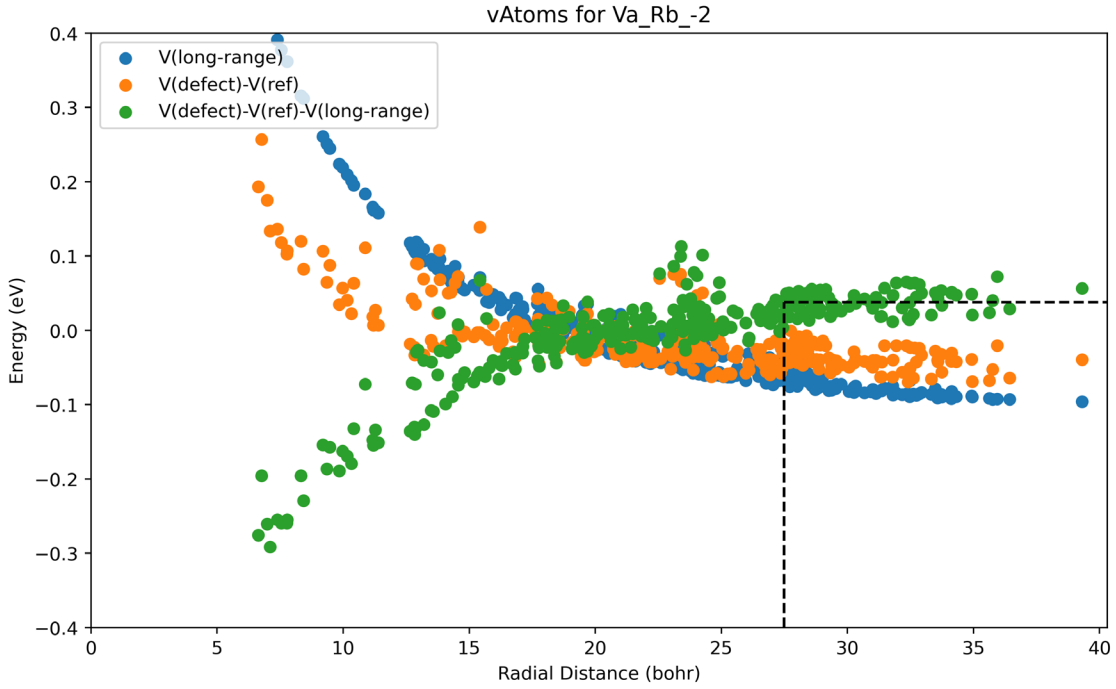

b. Zero Kelvin Approximation

When comparing our theoretical calculations with experiment, an important distinction is that our calculations are for the lattice at zero Kelvin. All atoms are relaxed until their motion stops. On the other hand, the experiments we compare with occur at room temperature or higher. Thermal motion effects and phonon effects are ignored in calculations. We expect phonon and zero-point effects to increase calculated luminescence energies, E_{lum}^{th}. We estimate this effect to be less than 0.1 eV.

Also, the band gap is typically smaller at room temperature versus zero kelvin. For instance, the band gap of silicon (GaN) varies from 1.17 (3.5) eV and 0K to 1.12 (3.5) at 300K. The shift is not known for $Rb_3Sb_2I_9$ but is expected to be between less than 0.1 eV and is split between a valence band and conduction band shifts. The effect on our calculations of a lower room temperature band gap depends on the shift of the gap defect levels which are expected to be smaller than the gap shift. Overall, we estimate this effect to be less than 0.05 eV.

Figure S2. Electronic Structure of $P2/n_1$ $Rb_3Sb_2I_9$ The band structure plot of $Rb_3Sb_2I_9$ using the PBEsol functional is reported in the left panel. The respective electron density of states are reported in the right panel. The high symmetry points in reciprocal lattice units are Z=[0.0, 0.5, 0.0], D =[0.0, 0.5, 0.5], and B = [0.0, 0.0, 0.5]

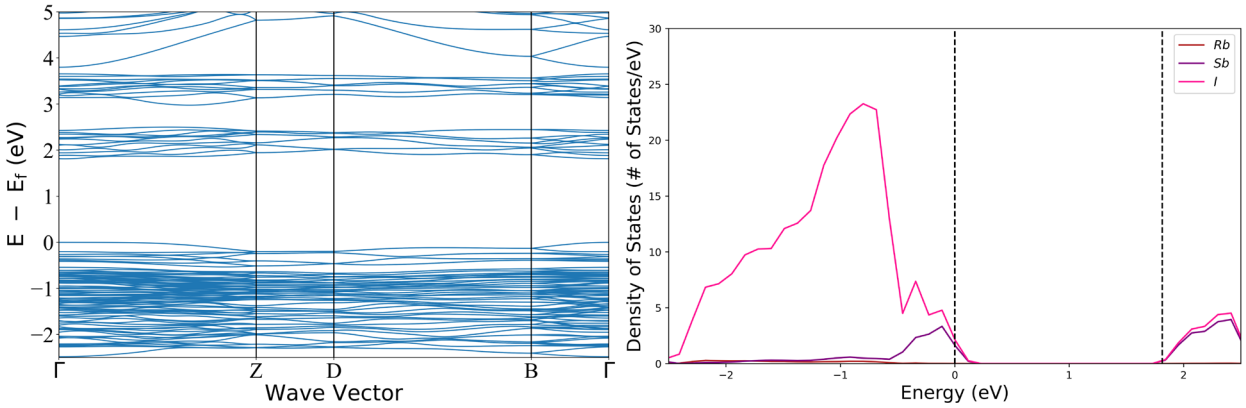
E − E_f (eV)
5
4
3
2
1
0
−1
−2
Γ
Z
D
B
Γ
Wave Vector
Density of States (# of States/eV)
30
25
20
15
10
5
0
−2
−1
0
1
2
Energy (eV)
Rb
Sb
I

Figure S3: Phase Stability Diagrams: The chemical potentials in the plot below are the same as the $\Delta\mu$ values defined in the main text. The $Rb_3Sb_2I_9$ stability (A,B,C,D) region below corresponds to the green region shown in **Figure 2** of the main text. The results are from pydefect[29] using hybrid HSE-SOC calculations for the top figure S3a and semi-local PBEsol for the bottom figure S3b. Notice the two results are very similar indicating semi-local functionals do well for the bulk energies of these Rb, Sb, and I containing solid materials. The corners of the stability region for $Rb_3Sb_2I_9$ are given can be written in terms of the $(\Delta\mu_{Rb}, \Delta\mu_{Sb}, \Delta\mu_I)$ values (in eV) which are for points A, B, C and D equal to (-3.364, -1.410, -0.013), and (-3.140, -1.410, -0.088), (-2.894, 0.0, -0.483), and (-2.670, 0.0, -0.558), respectively, for Figure S3a, and (-3.059, -1.266, -0.021), and (-2.880, -1.266, -0.081), (-2.637, 0.0, -0.443), and (-2.458, 0.0, -0.503), respectively, for Figure S3b.

a)

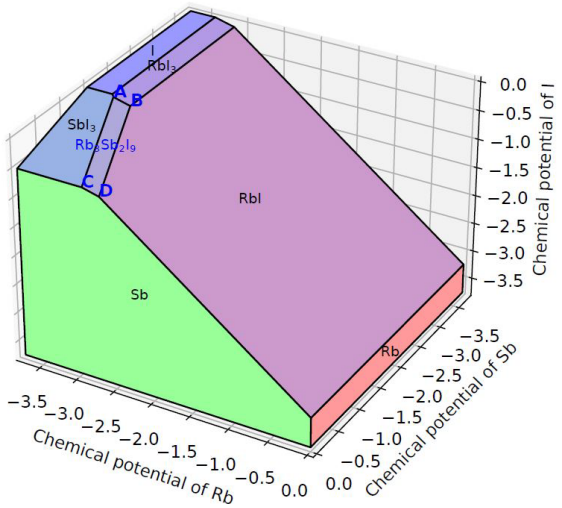

b)

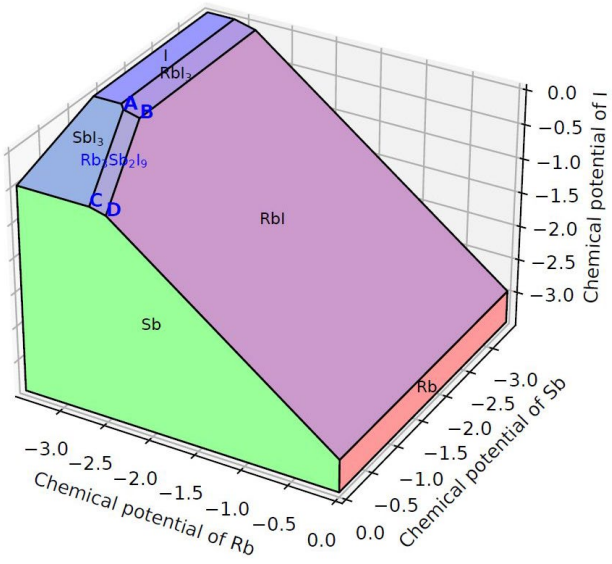

Figure S4: Formation energies versus Fermi energy for two supercell. The figures below report PBEsol energies from the 3x2x1 supercell calculations. The chemical potential values $(\Delta\mu_{Rb}, \Delta\mu_{Sb}, \Delta\mu_{I})$ for the left and right figure below corresponds to points A and D, respectively, of the phase stability plot (supplemental **Figure 3b**). The right plot has the same results as **Figure 7** of the main text, expect this plot also includes the anti-site defects.

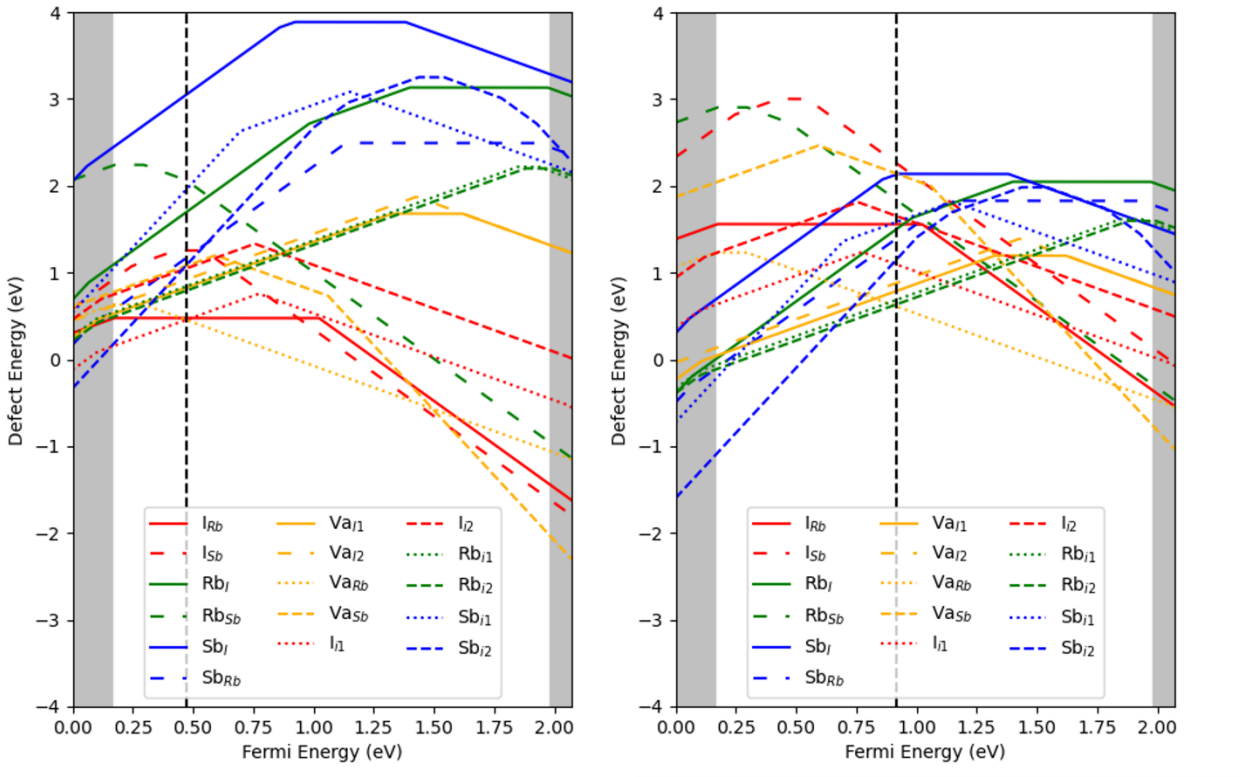

Figures S5: Configuration Coordinate Diagrams for Vacancy Type 1 Configuration coordinate diagram for iodine vacancy of type 1 with the defect reference state having neutral charge for (a) an extra electron in the valence band maximum energy state (e_vbm). The dots are calculated data points which are smoothly fit with a 2^{nd} order polynomial shown as the solid curves. Energies are calculated for 1x2x1 supercells using the PBEsol method (HSE-SOC versions are shown in the main text **Figure 9**).

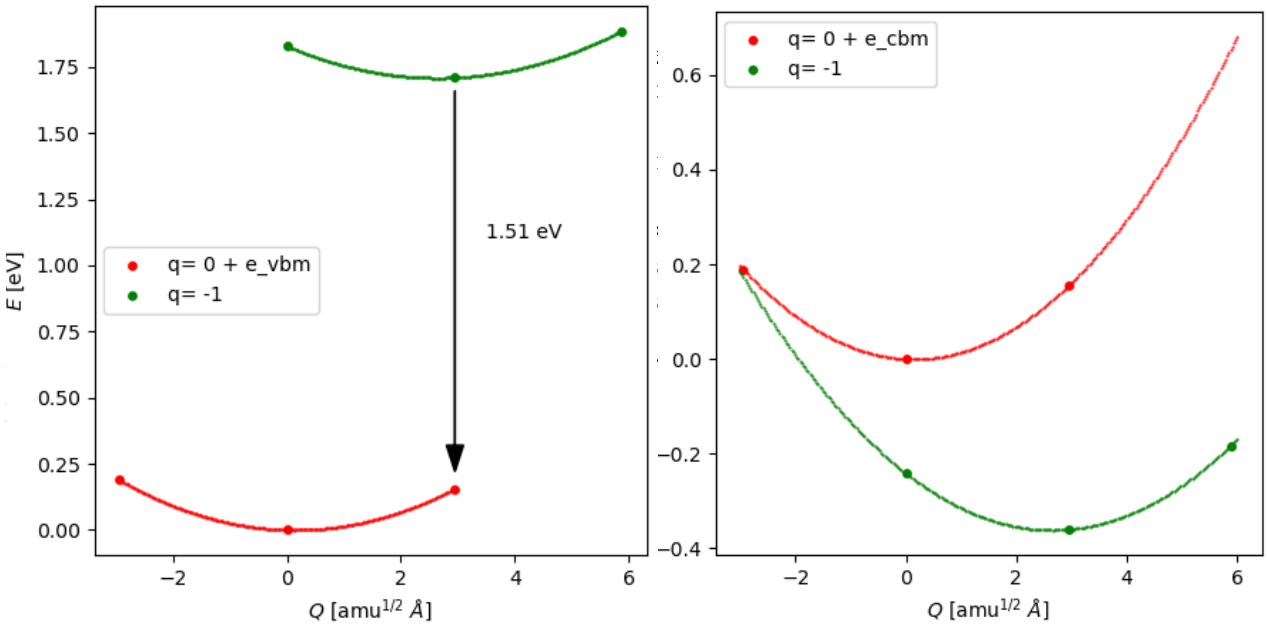

Figures S6: Configuration Coordinate Diagrams for Vacancy Type 1 Configuration coordinate diagram for iodine vacancy of type 1 with the defect reference state having $q = +1$ charge and an extra electron in the valence band maximum energy state (e_vbm). The dots are calculated data points which are smoothly fit with a 2^{nd} order polynomial shown as the solid curves. Energies are calculated for 1x2x1 supercells using the HSE-SOC method.

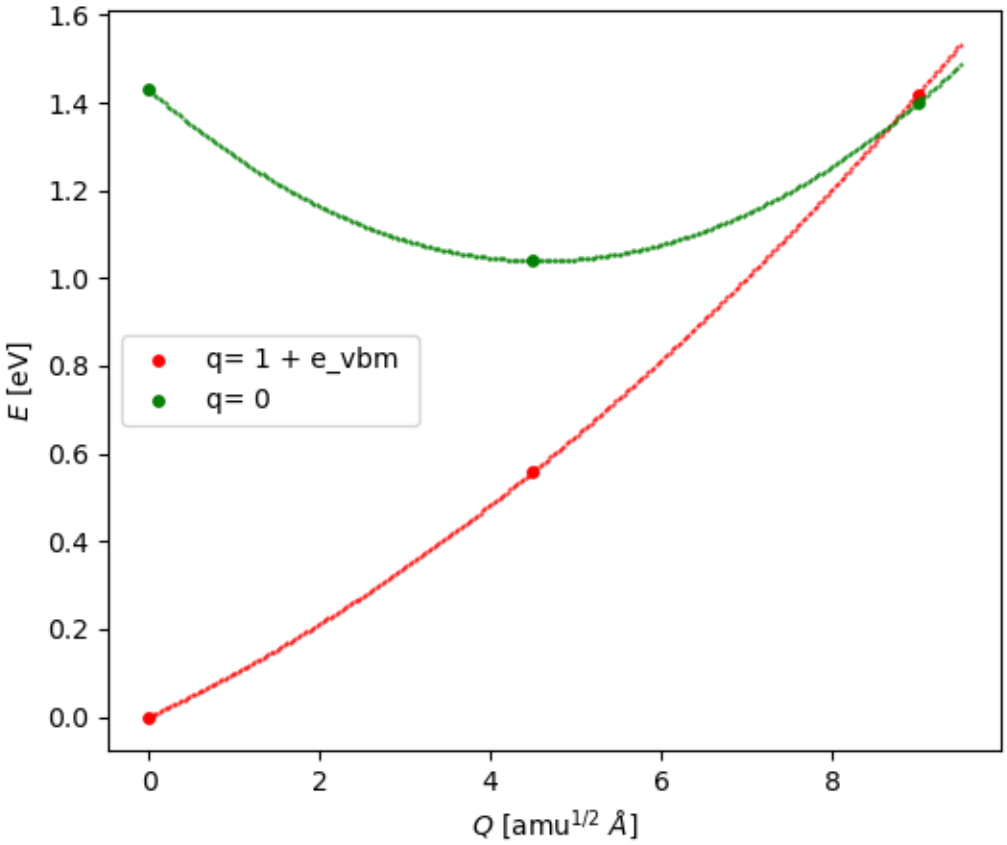

S7: Configuration Coordinate Diagrams for iodine at a rubidium site

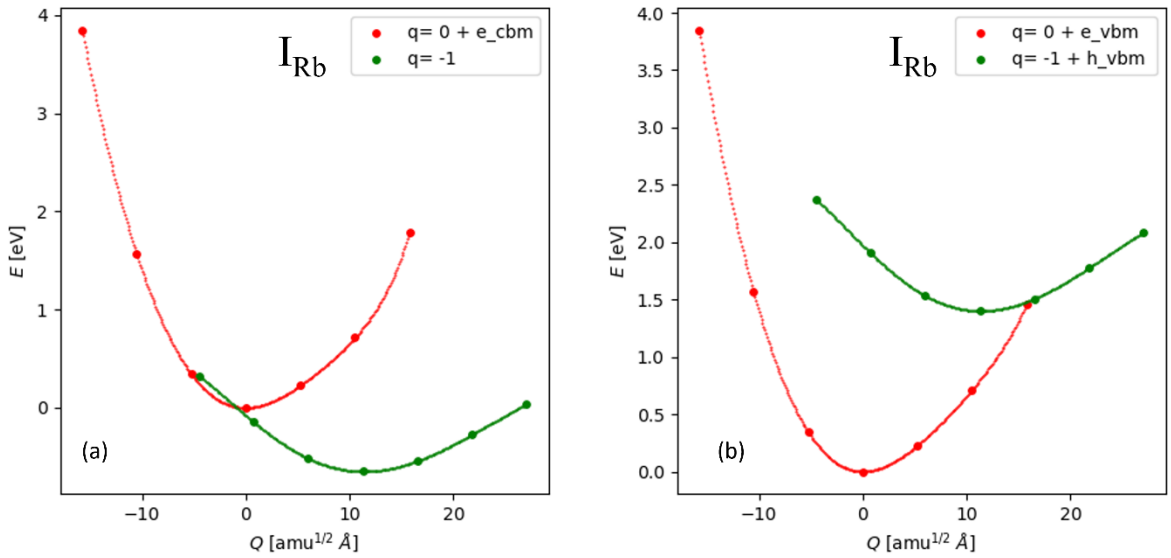

Figure S6: Configuration coordinate diagram for iodine substitution at a rubidium site (I_{Rb}) with the defect reference state having neutral charge for (a) an extra electron in the conduction band minimum state (e_cbm) and (b) the extra electron is in the valence band maximum state (e_vbm).

The I_{Rb} defect prefers the neutral charge state for typical Fermi levels based on charge neutrality conditions. With large numbers of electrons and holes, **Figure S7(a)** shows that the neutral defect will trap an electron through a barrierless non-radiative process. **Figure S7(b)** shows the negatively charged I_{Rb} defect traps a hole with very small barrier ($< 0.1\ eV$). Therefore, I_{Rb} defects should significantly reduce the free carrier concentration in a photoconductivity experiment or during an optoelectronic device's operation, but they may not hold trapped charges long enough to be observed experimentally.